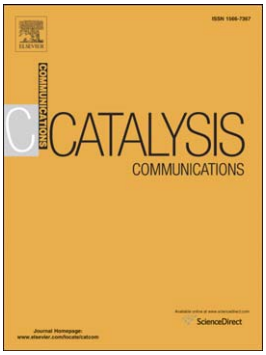


# Hydrolytic hydro-conversion of cellulose to ethylene glycol over bimetallic CNTs-supported NiWB amorphous alloy catalyst

Haili Liu, Lin Qin, Xiaoyue Wang, Changhai Du, De Sun, Xiangchun Meng

PII: S1566-7367(16)30013-9
DOI: doi: 10.1016/j.catcom.2016.01.014
Reference: CATCOM 4559

To appear in: *Catalysis Communications*

Received date: 31 August 2015
Revised date: 10 January 2016
Accepted date: 15 January 2016

Please cite this article as: Haili Liu, Lin Qin, Xiaoyue Wang, Changhai Du, De Sun, Xiangchun Meng, Hydrolytic hydro-conversion of cellulose to ethylene glycol over bimetallic CNTs-supported NiWB amorphous alloy catalyst, *Catalysis Communications* (2016), doi: 10.1016/j.catcom.2016.01.014

To be submitted to Catalysis Communications

# Hydrolytic hydro-conversion of cellulose to ethylene glycol over bimetallic CNTs-supported NiWB amorphous alloy catalyst

Haili Liu, Lin Qin, Xiaoyue Wang, Changhai Du*, De Sun, Xiangchun Meng

*School of Chemical Engineering, Changchun University of Technology, Changchun 130012, Jilin, P .R.. China*

* Corresponding author. Tel.: +86 431 85716461
*E-mail address*: du661123@163.com

## Abstract

NiWB/CNTs catalysts were prepared by ultrasonic impregnation chemical reduction method and showed high activity in the hydrolytic hydro-conversion of cellulose to ethylene glycol. The conversion of cellulose could be high to 100 % with an ethylene glycol selectivity of 57.7 %. The catalysts were characterized by XRD, TEM, $NH_3$-TPD and XPS. The hydrolytic hydro-conversion activity of the catalyst was related to it's highly dispersion of NiWB, appropriate particle size and the synergistic effect between strong acid sites in CNTs and NiW alloying structure.

**Keywords:** Cellulose, NiWB/CNTs catalyst, Catalytic hydrogenation, Ethylene Glycol

## 1. Introduction

Cellulose is the most abundant source of biomass, and holds impressive potential as an alternative to fossil fuels for sustainable production of fuels and chemicals [1-4]. Various processes have been employed to convert cellulose biomass into fuels and chemicals [5-8]. One-pot conversion of cellulose with solid catalysts via hydrolytic hydrogenation is a green process for the sustainable production of polyols. Fukuoka et al. reported firstly that cellulose can be directly converted into hexitols over $Pt/Al_2O_3$ catalyst and the yield of hexitols was around 30 % [9]. Recently, carbon has been advocated as a leading material for chemical biomass transformation process due to its large specific surface area, high porosity, excellent electron conductivity, and relative chemical inertness [10]. Luo et al. used a carbon supported Ru catalyst for the hydrogenolysis of cellulose and obtained a 39.3 % yield of hexitols [11]. Deng et al. investigated the use of Ru supported on carbon nanotubes (CNTs) for cellulose conversion, and a 40% yield of hexitols could be achieved [12]. Van de Vyver et al. presented a study wherein Ni supported on carbon nanofibers (CNFs) was used. Under the applied reaction conditions, a 76 % yield in hexitols with 69 % sorbitol selectivity at 93 % conversion of cellulose was obtained [13]. Interestingly, Zhang and co-workers developed a series of tungstenic catalysts including Ni-$W_2C$/AC, WC/MC and Ni-W/SBA-15, which can effectively catalyze the conversion of cellulose into polyols and the yield of ethylene glycol (EG) was as high as 61-75 wt% [14-16]**.** Others recently reported the use of metallic tungsten and tungsten oxide based dual-functional catalysts for the cellulose conversion to EG [17-19]. All these findings opened the way for other combinations of hydrogenation catalysts and tungsten-based catalysts for the production of bulk valuable EG from biomass [20-22].

Amorphous catalyst possesses some interesting and intrinsic properties such as a microstructure of long-range disorder and short-range order [23-26], leading to its excellent activity in the catalytic hydrogenation reactions [27-31]. However, to our knowledge, it has not been examined for the conversion of cellulose. In the present work, a series of NiWB/CNTs amorphous catalysts were prepared by chemical reduction method, and were used in the conversion of cellulose into polyols.

## 2. Experimental

### 2.1. Catalyst preparation

CNTs were pretreated in concentrated $HNO_3$ (33 wt %) at 80 ℃ under refluxing conditions to remove amorphous carbon. The purified CNTs were impregnated by a 0.1 mol/L NaOH solution of $Ni(NO_3)_26H_2O$ and ammonium metatungstate and were sonicated for 0.5 h. After being kept at room temperature for 12 h, the mixture was reduced by adding dropwise 0.5 mol/L $NaBH_4$ with the solution of 0.1 mol/L NaOH. The resulting catalyst was washed thoroughly with distilled water and anhydrous ethanol. The as-prepared sample was denoted as x % NiWB (y)/CNTs where x represented the theoretical weight percentage of Ni and W in catalyst: x = (Ni+W) / (Ni+W+CNTs) × 100, and y represented the mole ratio of Ni and W.

### 2.2. Catalyst characterization

XRD measurements were recorded using a Siemens D500 powder diffractometer with Al Kα radiation (40 kV, 30 mA). The surface morphology was characterized by TEM (JEOL JEM2011). The XPS spectra were recorded using Perkin Elmer PHI 5000C instrument. $NH_3$-TPD was performed by using a Micromeritics Autochem 2920 Ⅱinstrument.

### 2.3. Catalytic experiments

0.5 g microcrystalline cellulose (crystallinity 85 %, Alfa Aesar), 0.15 g NiWB/CNTs and 15 mL deionized water were put into a 50 mL stainless steel autoclave and heated to the reactor to the preset temperature and then hydrogen was filled into the reactor with preset pressure. After reaction, the products were analyzed by a HPLC system (Shimadzu LC-20AB) equipped with RI detector and an USPpak MN-431 column.

## 3. Results and discussion

### 3.1. Catalyst characterization

Fig.1 shows the TEM image for the 30 % NiWB(1:1)/CNTs catalyst. From the TEM image, we can see that NiWB particles appear to be well distributed over the CNTs surface, and a rather broad distribution of the NiWB particle sizes centered around 15 nm. The SAED

picture (inset in Fig.1) revealed that the fresh NiWB nanoparticles displayed diffraction circle characteristic of amorphous structure [23]. TEM images of other NiWB/CNTs catalysts show that NiWB particles on 20 % NiWB(1:1)/CNTs, 25 % NiWB(1:1)/CNTs and 35 % NiWB(1:1)/CNTs centered around 45 nm, 30 nm and 32 nm respectively (Figure S1 in SI). The relatively large particles could be attributed to particle agglomeration.

XRD patterns are shown in Fig.2. Only one broad peak around 2θ=45° appeared in Fig. 2 (a), indicating that the fresh NiWB sample pretreated at room temperature had a typical amorphous structure [32, 33]. After the sample was treated at 473 K, the broad peak was not observed, and intensive peaks at 2θ=45°, 52° appeared in the XRD pattern, attributing to Ni(111) and Ni(200), respectively, indicating that Ni metal particle formed. There are three diffraction peaks at around 26.5°, 43.16° and 53.2° appeared in Fig. 2 (b) that could be assigned to the diffraction peaks of C(002), (100) and (004), respectively [34]. No any amorphous NiWB diffraction peak could be observed, which indicates that NiWB exists in the very small nanoparticle and highly dispersed on the CNTs surface. No obvious intensive peaks of Ni were observed for the 30 % NiWB(1:1)/CNTs samples up to 573 K, it could be concluded that the thermal stability of the 30 % NiWB(1:1)/CNTs catalyst was higher than that of NiWB.

The $NH_3$-TPD profiles of desorbed ammonia ($NH_3$) on various samples of catalyst are shown in Fig.3. The profiles of all the catalysts displayed a very broad desorption peaks, which is indicative of acid site heterogeneity [35]. All catalysts showed two distinct peaks appearing from 380 ℃ to 460 ℃ and 550 ℃ to 800 ℃, attributing to medium-strength and strong acid sites, respectively.

To unravel the nature of the acidity, $NH_3$-TPD was performed to inspect the difference in acidity generated on CNTs support, NiWB and NiWB/CNTs samples (Fig. 4.). For the CNTs support untreated with $HNO_3$, no any acidic sites were observed. But for the CNTs pre-treated with 33% $HNO_3$, a broad peak at 550-800 ℃ was observed, suggesting the generation of medium-strength and strong acid sites on its surfaces. It is known that the treatment of carbon materials by $HNO_3$ can cause the generation of acidic groups such as carboxylic groups on their surfaces [12, 13]. The $NH_3$-TPD profile associated with the NiWB sample reveals the presence of two desorption peaks. While the peak centered at 400-450 ℃ ascribed to

medium-strength acidic sites, the broad signal in the temperature range between 600 ℃ and 750 ℃ is assigned to the presence of strong acid sites. For 30 % NiWB(1:1)/CNTs catalyst, the strong acid sites and a large acid amounts over the temperature range from 550 ℃ to 800 ℃ were detected, which attributed to the synergistic effect between acidic groups in CNTs support and $WO_3$ species (as discussed below) in NiWB.

The XPS spectra of Ni, W and B in the NiWB/CNTs catalysts are shown in Figure S2. Compared with standard binding energies of elemental Ni (853.0 eV), B (187.0 eV) and W (31.0 eV) [18, 36-37]. The peak of Ni $2p_{3/2}$ electron binding energy was found to be at 856.0 eV, indicating that nickel existed as oxidized nickel both in NiWB/CNTs and NiWB samples, and the peak around 861.5 eV was ascribed to $Ni(OH)_2$ (electron shakeup) [38]. Because the catalyst preparation was carried out in the aqueous solution without the nitrogen protection, Ni is in its oxidized form. However, metallic Ni is needed for the hydrogenation reactions. In order to confirm that metallic Ni is the active specie for the reaction, a substrate-blanc reaction (just water, catalyst and $H_2$) was performed on 30 % NiWB(1:1)/CNTs under identical conditions (at 523 K and 6 MPa $H_2$ ). XPS spectra showed that the peak at 853.1 eV was attributed to metallic Ni while the peak at 858.3 eV was ascribed to the Ni electron energy-loss peak [39-40] (Figure S3 in SI). There were two peaks in the B 1s spectra: The peak near 187.0 eV was attributed to elemental B, and the peak near 192.5 eV was attributed to boron oxide. It was noticed that the intensity of the elemental B and boron oxide peaks increased dramatically in the presence of CNTs support. With the introducing of CNTs support, the peak of B 1s binding energy of elemental B shifted from 187.3 eV to 186.6 eV, implying that CNTs support could restrain the electron donation of elemental B to the other elements, compared to that in the unsupported NiWB. Such a phenomenon implies that some alloying structure may have formed between Ni and W, which is essential for the improvement of the catalytic activity of NiWB/CNTs to that of NiWB shown below. The W 4f XPS spectrum was deconvoluted into three peaks. The peaks around 35.0 and 37.0 eV were attributed to W $4f_{7/2}$ and W $4f_{5/2}$ doublets, respectively, of $WO_3$ [33, 40], indicating that $W^{6+}$ could not be reduced by $NaBH_4$ and existed in the form of oxide. The NiW loading on CNTs, the bulk composition, surface composition and the relative content of element with different valences are shown

in Table S1. The NiW loading on CNTs is approximately close to the theoretical value, and the bulk composition of all samples was similar. However, the Ni atom content on the catalyst surface was much larger than that of the corresponding bulk composition.

3.2. Catalytic performance

The conversion and products selectivity in the hydrolytic hydro-conversion of cellulose to ethylene glycol over various solid catalysts are shown in Table 1. In the cases in which no catalyst was used (Table 1, entry 1), or CNTs-untreated by $HNO_3$ (Table 1, entry 2) was used, no polyols were observed. Although conversions of cellulose were about 65 %, the cellulose appeared to be converted into cello-oligomers [11]. When CNTs-pretreated by $HNO_3$ was used (Table 1, entry 3), EG was obtained with a yield of 4.2 % at a cellulose conversion of 71.6 % due to CNTs's acidic groups and its hydrogen spillover [10].

As shown in Table 1, various supported catalysts gave different catalytic performances. 30 % NiWB (1:1) / CNTs showed the highest EG yield of 57.7 % at a cellulose conversion of 100 % (Table 1, entry 11), which was higher than that of $WO_3$+Ru/C catalyst (Table 1, entry 16) and Ni/AC+W/AC catalyst (Table 1, entry 17). This might be related to the synergistic effect between strong acid sites in CNTs support and NiW alloying structure.

The effect of different loadings of NiWB was investigated. When the NiWB loading was changed from 20 % to 30 %, the cellulose conversion increased from 75.4 % to 100 % with a concurrent increase in the yield of EG from 18.8 % to 57.7 % (Table 1, entry 15, 14, and 11). The gas phase analysis showed that a small amount of CO, $CO_2$ and $CH_4$ were produced (Table S2 in SI). TEM characterization shows that these catalysts have different size distributions of NiWB particles with diameter of 45, 30, and 15 nm from 20 % to 30 % loading, indicating that NiWB particle size for the cellulose hydrogenation is important. For NiWB catalyst, the EG yield was relatively high, at 43.2 % with a cellulose conversion of 100 %, which the EG yield was lower than that of 30 % NiWB (1:1) / CNTs. The TEM image of NiWB (Fig. S4 in SI) shows that shapeless particles with a broad distribution of particle size, from 20 nm to 90 nm, were present. The relatively large

particles could be attributed to particle agglomeration.

It had been reported that the conversion of cellulose to polyols involves hydrolysis of cellulose by inorganic acids to glucose, and subsequent hydrogenation of glucose to sorbitol and other polyols [41, 42]. $NH_3$-TPD results show that all NiWB/CNTs catalysts have medium-strength and strong acid sites. W in NiWB/CNTs amorphous catalysts was in form of $WO_3$, which was a good Brönsted acid site [33]. The highly dispersed $WO_3$ species are active mainly as solid acid for the hydrolysis of cellulose to glucose, and also catalyze the cleavage of the C-C bonds in glucose [18], which may form glycolaldehyde and erythritol, the possible intermediate, for EG formation [21, 22]. Accordingly, a possible reaction pathway over NiWB/CNTs catalyst is proposed (Scheme 1). In light of the reaction pathway, the retro-aldol activity is attributed to the tungsten component of the catalyst and the hydrogenation activity is associated with the metallic Ni of the catalyst. Under the high temperature （523 K）hydrothermal conditions applied in this work, the tungsten species can be transformed into $H_xWO_3$ by $H_2$ [20], and the dissolved $H_xWO_3$ may be the genuinely catalytically active species in the retro-aldol reaction. However, more fundamental studies are required to support this hypothesis.

Table 2 shows the surface compositions and recycling results during hydrolytic hydro-conversion of cellulose over 30 % NiWB(1:1)/CNTs. The conversion of cellulose decreased gradually to 79.5 %, and the selectivity to ethylene glycol was 10.6 % after 5 runs. The decrease of activity might be attributed to the crystallization of the NiWB/CNTs catalyst, as revealed by XRD pattern of the used sample (Fig. S5 in SI). It was difficult to separate the NiWB/CNTs catalysts mixed with solid cellulose in this case. However, from the atomic ratio, it can be observed that the Ni/W and Ni/W+B atomic ratio decreased after 5 runs, indicating the leaching of Ni specie in hot-compressed water.

## 4. Conclusions

The amorphous NiWB/CNTs catalyst prepared by chemical reduction method showed high activity in the hydrolytic hydrogenation of commercial microcrystalline cellulose, giving a maximum yield of ethylene glycol being 57.7 %. The catalytic activity can be attributed to the highly dispersion of NiWB in the CNTs support, appropriate particle size and the

synergistic effect between strong acid sites in CNTs and NiW alloying structure.

**Acknowledgements**

This work was supported by the Key Scientific and Technological Project Foundation of Jilin Provincial Science and Technology Department, China (20150204031GX) and the Scientific Research Fund of Jilin Provincial Education Department, China (2014126).

**References**

[1] G. W. Huber, S. Iborra, A. Corma, Chem. Rev. 106(2006)4044-4098.

[2] A. M. Ruppert, K. Weinberg, R. Palkovits, Angew. Chem. Int. Ed. 51 (2012) 2564-2601.

[3] S. Van de Vyver, J. Geboers, P. A. Jacoks, B. F. Sels, ChemCatChem. 3 (2011) 82-94.

[4] M. Dusselier, M. Mascal, B. F. Sels, Top. Curr. Chem. 353 (2014) 1-40.

[5] J. Carlos Serrano-Ruiz, R. M. West, J. A. Dumesic, Annu. Rev. Chem. Biomol. Eng. 1(2010)79-100. .

[6] D. M Alonso, S. G. Wettstein, J. A. Dumesic, Chem. Soc. Rev. 41(2012)8075-8098.

[7] S. Suganuma, K. Nakajima, M. Kitano, D. Yamaguchi, H. Kato, S. Hayashi, J. Am. Chem. Soc. 130(2008) 12787-12793.

[8] M. Mascal, E. B. Nikitin, ChemSusChem. 3(2010)1349-1351.

[9] A. Fukuoka, P. L. Dhepe, Angew. Chem. Int. Ed.45(2006)5161-5163.

[10] E. Lam, John H. T. Luong, ACS Catal. 4 (2014) 3393-3410.

[11] C. Luo, S. Wang, H. Liu, Angew. Chem. Int. Ed.46 (2007) 7636-7639.

[12] W. P. Deng, X. S. Tan, W. H. Fang, Q. H. Zhang, Y. Wang, Catal. Lett. 133(2009)167-174.

[13] S. Van de Vyver, J. Geboers, W. Schutyser, M. Dusselier, P. Eloy, E. Dornez, J. Won Seo, C. M. Courtin, E. M. Gaigneaux, P. A. Jacobs, B. F. Sels, ChemSusChem. 5 (2012) 1549-1558.

[14] N Ji, T Zhang, M. Y. Zheng, A. Q. Wang, H. Wang, X. D. Wang, J. G. Chen, Angew. Chem. Int. Ed. 47(2008)8510-8513.

[15] L. N. Ding, A. Q. Wang, M. Y. Zheng, T. Zhang, ChemSusChem. 3 (2010)818-821.

[16] Y. Zhang, A. Wang, T. Zhang, Chem. Commun. 46(2010)862-864.

[17] M. Y. Zheng, A. Q. Wang, N. Ji, J. F. Pang, X. D. Wang, T. Zhang, ChemSusChem. 3 (2010) 63-66.

[18] Y. Liu, C. Luo, H. Liu, Angew. Chem. Int. Ed 51(2012) 3249-3253.

[19] Z. J. Tai, J. Y. Zhang, A. Q. Wang, M. Y. Zheng, T. Zhang, Chem. Commun. 48 (2012) 7052-7054.

[20] A. Q. Wang, T. Zhang, Acc. Chem. Res. 46 (2013) 1377-1386.

[21] G. H. Zhao, M. Y. Zheng, J. Y. Zhang, A. Q. Wang, T. Zhang, Ind. Eng. Chem. Res. 52 (2013) 9566-9572.

[22] R. Ooms, M. Dusselier, J. A. Geboers, B. Op de Beeck, R. Verhaeven, E. Gobechiya, J. A. Martens, A. R. Redl, B. F. Sels, Green Chem. 16 (2014) 695-707.

[23] H. Li, H. Li, J. Zhang, W. Dai, M. Qiao, J. Catal. 246(2007) 301-307.

[24] H. Li, D. Zhang, G. Li, Y. Xu, Y. Lu, H. Li, Chem. Commun. 46(2010)791-793.

[25] M. Mo, L. Han, J. Lv, Y. Zhu, L. Peng, X. Guo, W. Ding, Chem. Commun. 46(2010)2268-2270.

[26] H. Li, D. Chu, J. Liu, M. Qiao, W. Dai, H. Li, Adv. Synth. Catals. 350(2008) 829-836.

[27] Á. Molnár, G. V. Smith, M. Bartók, Adv. Catal. 36 (1989) 329-383.

[28] X. Y. Ma, D. Sun, F. W. Zhao, C. H. Du, Catal. Commun. 60 (2015) 124-128.

[29] G. Luo, S. Yan, M. Qiao, J. Zhuang, K. Fan, Appl. Catal. A: Gen. 275(2004) 95-102.

[30] W. Wang, Y. Yang, H. Luo, H. Peng, F. Wang, Ind. Eng. Chem. Res. 50(2011) 10936-10942.

[31] S. E. Skrabalak, K. S. Suslick, Chem. Mater. 18 (2006) 3103-3107.

[32] G. L. Parks, M. L. Pease, A. W. Burns, K. A. Layman, M. E. Bussell, X. Wang, J. Hanson, J. A. Rodriguez, J. Catal. 246(2007)277-292.

[33] W. Wang, Y. Yang, H. Luo, H. Peng, B. He, W. Liu, Catal. Commun. 12(2011) 1275-1279.

[34] H. J. Wang, L. L. Zhu, S. Peng, F. Peng, H. Yu, J. Yang, Renew. Energ. 37(2012)192-196.

[35] L. C. Peng, L. Lin, J. H. Zhang, J. B. Shi, S. J. Liu, Appl. Catal. A: Gen. 397(2011)259-265.

[36] K. Lian, D. Kirk, S. Thorpe, J. Electrochem. Soc. 142(1995)3704-3712.

[37] J. H. Shen, Y.W. Chen, J. Mol. Catal. A: Chem. 273(2007)265-276.

[38] W. L. Dai, M. H. Qiao, J. F. Deng, Appl. Surf. Sci. 120(1997)119-124.

[39]T. Deng, J. Sun, H. Liu, Sci. China. Chem. 53(2010) 1476-1480.

[40]B. Zhao, C. J. Chou, Y.W. Chen, Ind. Eng. Chem. Res. 49(2010)1669-1676.

[41] R. Palkovits, K. Tajvidi, A. M. Ruppert, J. Procelewska, Chem. Commun. 47(2011)576-578.

[42] J. Geboers, S. Van de Vyver, K. Carpentier, P. Jacoks, B. Sels, Chem. Commun. 47(2011)5590-5592.

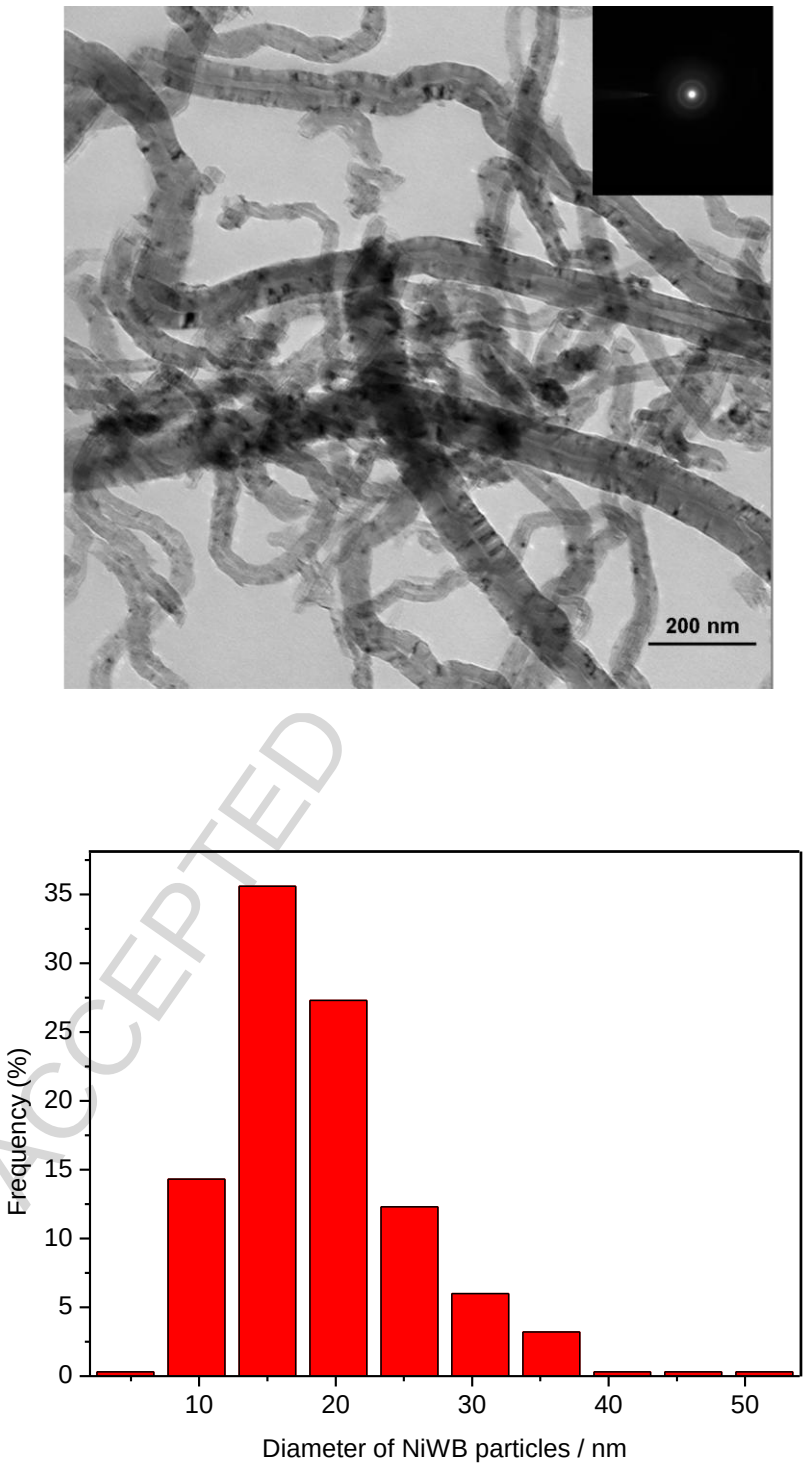


Fig.1. TEM image and the corresponding histogram of the NiWB particle size distribution of the 30 % NiWB(1:1)/CNTs catalyst.

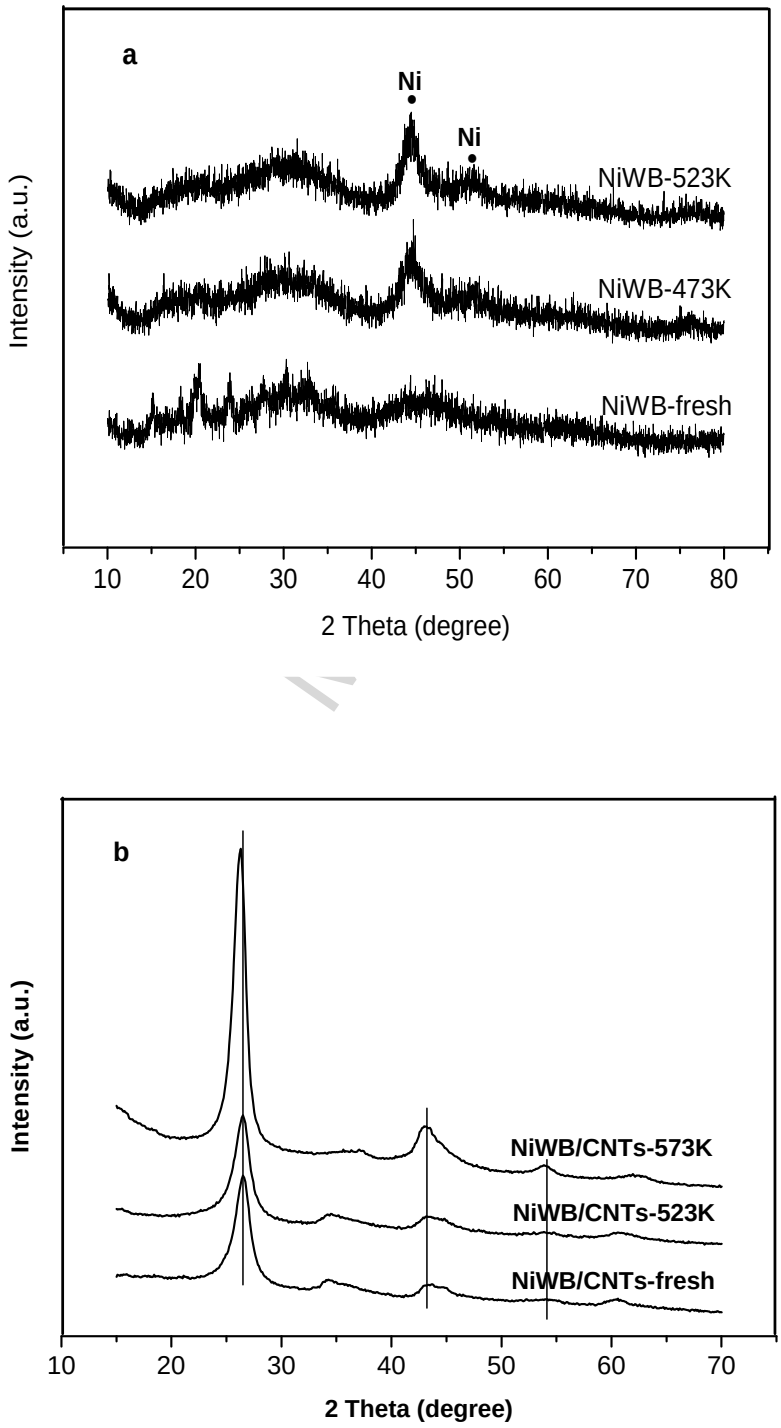


Fig.2. XRD patterns of (a) NiWB amorphous catalysts and (b) 30 % NiWB(1:1)/CNTs catalysts.

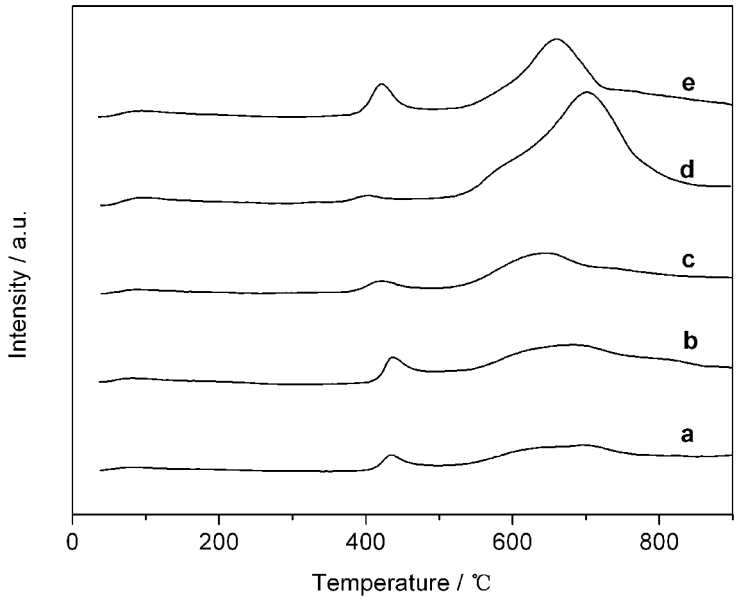


Fig.3. $NH_3$-TPD profiles for the NiWB/ CNTs catalysts with various NiWB loadings.

a—15 % NiWB(1:1)/CNTs, b—20 % NiWB(1:1)/CNTs, c—25 % NiWB(1:1)/CNTs, d—30 % NiWB(1:1)/CNTs, e—35 % NiWB(1:1)/CNTs.

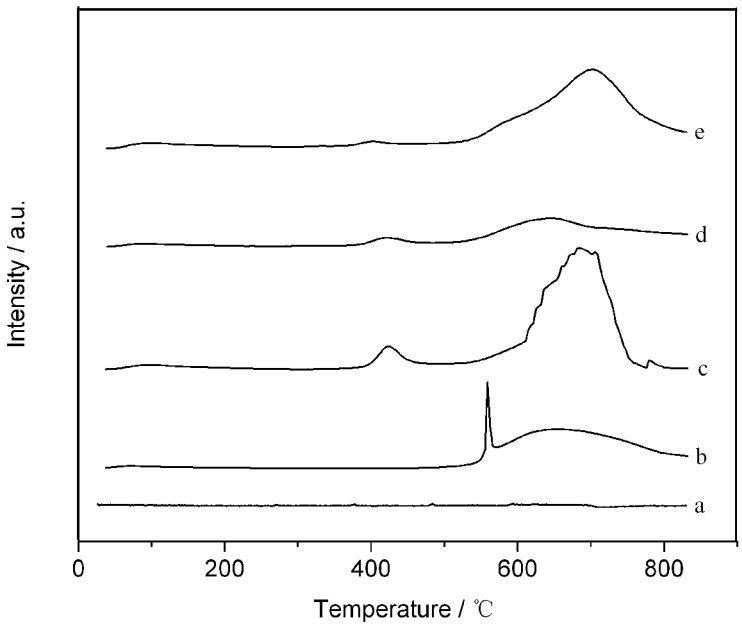


Fig.4. $NH_3$-TPD profiles of (a) CNTs-untreated with $HNO_3$, (b) CNTs-pretreated with 33% $HNO_3$, (c) NiWB catalyst, (d) NiWB/CNTs- untreated with $HNO_3$ and (e) NiWB/CNTs-pretreated with $HNO_3$.

**Table 1** Results of cellulose conversion and yields of main products[a].

| Entry | Catalyst | Cellulose conversion (%)[b] | Product yield based on carbon / % | | | | |
|---|---|---|---|---|---|---|---|
| | | | Ethylene glycol | Sorbitol | Mannitol | 1,2-propanediol | Others[c] |
| 1 | No catalyst | 64.3 | ---- | ---- | ---- | ---- | 64.3 |
| 2 | CNTs[d] | 65.7 | ---- | ---- | ---- | ---- | 65.7 |
| 3 | CNTs[e] | 71.6 | 4.2 | trace | trace | trace | 67.4 |
| 4 | NiWB (1:1) | 100.0 | 43.2 | 3.7 | 1.2 | 0.6 | 51.3 |
| 5 | 30 % NiWB (1:1)/AC | 85.1 | 27.6 | 24.6 | 6.71 | 2.4 | 23.8 |
| 6 | 30 % NiWB (1:1)/$SiO_2$ | 81.6 | 11.7 | 3.1 | 1.3 | 1.8 | 63.7 |
| 7 | 30 % NiWB (1:1)/$Al_2O_3$ | 76.6 | 0.4 | 4.0 | 1.1 | 2.1 | 69.0 |
| 8 | 30 % NiWB (1:1)/NaY | 81.6 | 11.3 | 2.6 | 1.5 | 1.9 | 64.0 |
| 9 | 30 % NiWB (3:1)/CNTs | 83.5 | 46.6 | 27.5 | 5.2 | trace | 4.2 |
| 10 | 30 % NiWB (2:1)/CNTs | 95.3 | 55.6 | 13.9 | 4.6 | 3.2 | 18.0 |
| 11 | 30 % NiWB (1:1)/CNTs | 100.0 | 57.7 | 7.1 | 3.2 | 4.6 | 27.4 |
| 12 | 30 % NiWB(0.5:1)/CNTs | 93.1 | 1.3 | 1.2 | 1.0 | 1.3 | 88.3 |
| 13 | 35 % NiWB (1:1)/CNTs | 98.5 | 44.4 | 14.0 | 2.3 | 3.4 | 34.4 |
| 14 | 25 % NiWB (1:1)/CNTs | 90.1 | 39.5 | 6.6 | 2.8 | 4.9 | 36.3 |
| 15 | 20 % NiWB (1:1)/CNTs | 75.4 | 18.8 | ND | 8.4 | 2.7 | 45.5 |
| 16[f] | $WO_3$+Ru/C[18] | 100.0 | 48.9 | 6.8 | 0.8 | 7.4 | ---- |
| 17[g] | Ni/AC+W/AC[17] | 100.0 | 46.6 | 2.5 | 5.9 | 8.0 | ---- |

[a] Reaction conditions: 523 K, $H_2$ 6 MPa (RT), cellulose 0.5 g, $H_2O$ 15 mL, reaction time 2 h, catalyst 0.15 g .

[b] Calculated by weight difference of solid cellulose before and after the reaction.

[c] Unidentified molecules including cello-oligomers and gaseous products.

[d] Untreated by $HNO_3$.

[e] Pretreated by 33% $HNO_3$.

[f] 518 K, 6 MPa $H_2$, 0.5 h.

[g] 518 K, 6 MPa $H_2$, 0.5 h.

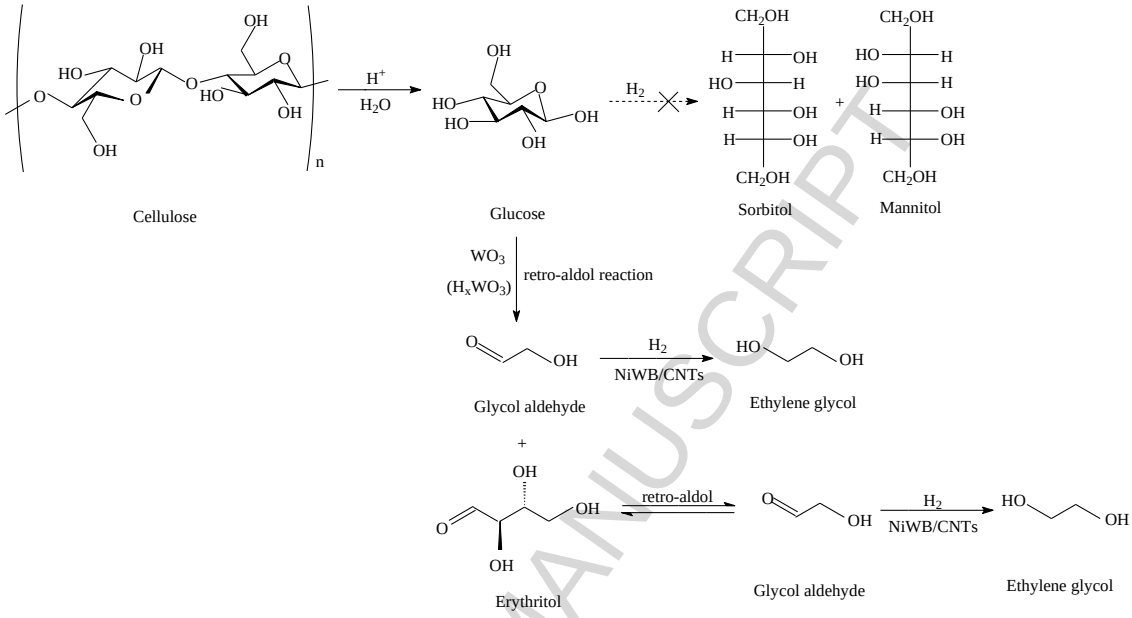


*Scheme 1.* Possible reaction pathway for catalytic conversion of cellulose into EG.

**Table 2** Surface compositions[a] and the conversion of cellulose and the selectivity of polyols as functions of cycle numbers over 30 % NiWB(1:1)/CNTs particle[b].

| Run numbers | Surface composition | Ni/W (atomic ratio) | Ni/(W+B) (atomic ratio) | Conversion / % | Selectivity / % | | |
|---|---|---|---|---|---|---|---|
| | | | | | EG | Sorbitol | Mannitol |
| 1 | $Ni_{80.29}W_{6.8}B_{12.91}$ | 11.81 | 4.07 | 100.0 | 57.7 | 7.1 | 3.2 |
| 2 | ---- | | | 100.0 | 51.4 | 2.4 | 1.9 |
| 3 | ---- | | | 92.3 | 48.2 | 1.3 | 1.2 |
| 4 | ---- | | | 80.1 | 12.4 | 0.4 | 0.1 |
| 5 | $Ni_{78.71}W_{11.45}B_{9.84}$ | 6.87 | 3.70 | 79.5 | 10.6 | 0.3 | 0.2 |

[a] Determined by XPS.

[b] Reaction conditions: 523 K, $H_2$ 6MPa, $H_2O$ 15 mL, reaction time 2 h.

Graphical abstract

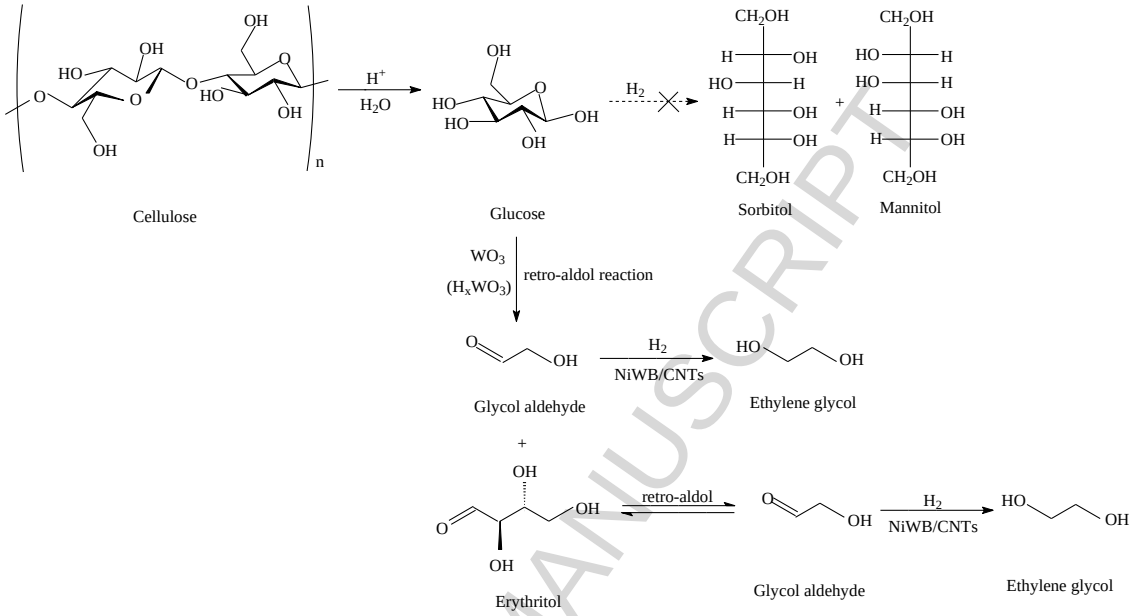


*Scheme 1.* Possible reaction pathway for catalytic conversion of cellulose into EG.

Highlights

- Catalytic conversion of cellulose into ethylene glycol with 57.7% yield on NiWB/CNTs.
- $WO_3$ species are active mainly as solid acid for the hydrolysis of cellulose to glucose.
- Strong acid sites and acid amounts are key factors.
- Catalytic performance depend on the NiWB alloy well distributed over the CNTs surface.